MSc in Photonics

Universitat Politècnica de Catalunya (UPC)
Universitat Autònoma de Barcelona (UAB)
Universitat de Barcelona (UB)
Institut de Ciències Fotòniques (ICFO)

PHOTONICS**BCN**

http://www.photonicsbcn.eu

Master in Photonics

MASTER THESIS WORK

BUILDING PLASMONIC CRYSTALS FROM PLASMONIC METAMOLECULES

David Enrique Medina Quiroz

Supervised by Dr./Prof. Agustin Mihi, ICMAB
And by Dr./Prof. Crina Cojocaru, UPC

Presented on date 9th September 2021

Registered at

Escola Tècnica Superior d'Enginyeria de Telecomunicació de Barcelona

Building Plasmonic Crystals from Plasmonic Metamolecules

DAVID ENRIQUE MEDINA QUIROZ[1,2,3]

[1] *Erasmus Mundus Joint Master Degree EUROPHOTONICS (2019-2021)*
[2] *Institute of Materials Science of Barcelona (ICMAB)*
[3] *david.enrique.medina@estudiantat.upc.edu*

Abstract: We present a theoretical and experimental analysis of the plasmon surface lattice resonances arising from gold nanoparticle assemblies. The metamolecules of the array are composed of colloidal gold nanoparticles and as the system is heated up, creating a single polycrystalline metamolecule. They were characterized by several microscopy methods for retrieving the shape. Subsequently, the optical resonances from the annealed plasmonic crystals were obtained by measuring the transmission at normal incidence and at several angles, and then compared to FDTD simulations for adjudicating field components to each resonance. Finally, photoluminiscence experiments were carried out in order to analyze the photoluminiscence enhancement and the potential applications for lasing.

Keywords– plasmonics, metamolecules, resonance, lattice, annealing, photoluminiscence.

1. Introduction

In recent years, there has been an impressive improvement in the fabrication techniques for nano-engineered materials. This has led to the design of materials with unconventional optical properties, which were, until this point, only described theoretically. Among them, we can name bound states in the continuum, Mie resonances and localized surface plasmons (LSP). LSPs are described as localized (non-propagating) excitations due the coupling of the oscillations of free electrons in metal nanostructures to an electromagnetic field [1]. They were mathematically established by Mie [2] more than 100 years and are nowadays studied experimentally for applications in areas such as sensing [3], lasing [4], imaging [5], photovoltaic devices [6], to name a few. However LSPs of single nanostructures are limited by the their low Q-factors [7], which are connected to the ratio of energy stored to the optical losses. This translates into a broad resonance peak. Hence, it makes it unsuitable for specific applications. However, these optical losses of the metal can be compensated by taking advantage of surface lattice resonances (SLR).

Nowadays, researchers are using metasurfaces as a novel approach to achieve resonances with high Q-factors since it is possible to confine electromagnetic modes in 1 or 2 dimensions within them. When metal nanostructures are arranged in periodic arrays, the influence of a single excitation influences the adjacent ones due to diffraction modes that emerge from Rayleigh-Wood anomalies. This leads to a plasmon surface lattice resonance (PSLR) [8] when the modes are coupled. Moreover, it has been proven that the PSLR is connected to the presence of hot spots in assemblies of nanoparticles [9]. The PSLR is narrowed down and red-shifted in comparison with localized resonance [10] and the frequencies at which PSLRs appear, depend on the particle shape and on the lattice parameters [11].

There have been different approaches to design suitable assemblies of gold nanoparticles that could yield PSLRs with sharp resonances. Building superlattices [12] by colloidal self-assembly is giving promising results as non-ordinary sharp resonances can arise due far-field effects. They can also be low-cost and easily fabricated by template assisted processes [13, 14].

When gold nanostructures are annealed, there will be a competition between coalescence and Ostwald rippening for the formation of new, more compact and polycrystalline structures [15, 16].

In addition, the annealing of nanoparticle assemblies results in metasurfaces yielding sharper resonances [15]. Thus, it would be interesting to do an in-depth analysis of superlattices with a later annealing process and look into its final shape and its optical properties.

In this work, we adopted a mixed approach by fabricating assemblies of colloidal nanoparticles with the same process presented by Matricardi et al. [14], in which we use a template-assisted self-assembly process that depends on the patterned polydimethylsiloxane (PDMS) mold for producing ordenated arrays from a colloidal solution. An annealing process was then developed for obtaining single metamolecules and enhancing the PSLR Q factor. We characterized the final shape of the metamolecules that compose the assembly by doing a correct theoretical comparison with the optical analysis. Finally, photoluminiscence experiments were carried out to take a closer look at the ratio of photoluminiscence enhancement (PLE) and their potential for applications in lasing.

2. Experimental methods

In this section we describe the methods of fabrication, characterization and of analysis used in this project. The first part focuses in the fabrication of the assemblies, the second on the characterization of the metamolecules shape and the last one in the methods used for the optical analysis.

2.1. Assembly fabrication

The assembly fabrication consists of two parts. First comes the fabrication of the colloidal gold nanoparticles assemblies and later the annealing process the assembly is put through.

2.1.1. Template assisted self-assembly

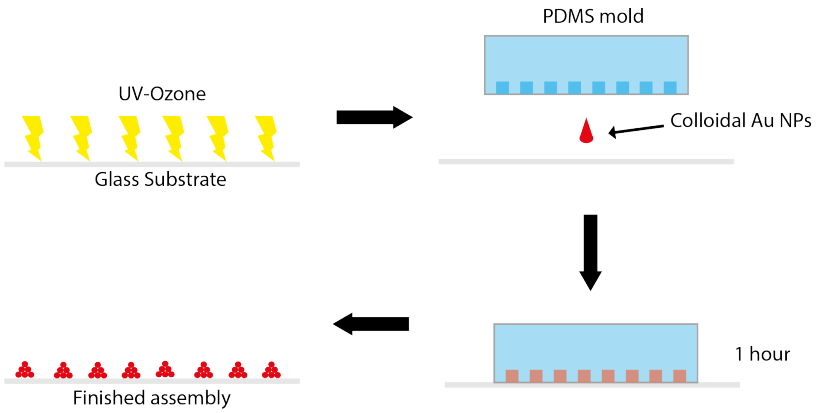

Fig. 1. Schematic of the template assisted self assembly using a soft lithography method.

The assemblies were fabricated using a template assisted method that consists in soft imprinting using polydimethylsiloxane (PDMS) molds. By the confinement of micro-scale volumes of a highly concentrated solution of nanoparticles between the substrate and the mold, the solvent evaporates and a self-assembly that replicates adequately the microcavities of the mold is developed. The molds were previously shaped with masters of patterns of holes with different lattice parameters (400, 500 and 600 nm) and a diameter of hole of approximately 200 nm 1. A glass substrate is first cleaned with soap, isopropanol, acetone and distilled water for a posterior UV-ozone treatment of 40 minutes for hydrolyzing the surface. By drop casting $1\mu l$ of

the colloidal solution of monodisperese gold nanoparticles of 25 nm of diameter, which were stabilized with polyethyleneglycol (PEG), and then pressing the mold into the substrate, we get the desired periodic pattern after waiting for the solvent to evaporate.

2.1.2. Annealing

As it was already demonstrated that the increase of crystallinity of the metamolecules improves the Q-factor [15]. For obtaining something similar, an attempt to anneal the resulting assemblies was done. The first annealing is done at 150°C (As at low annealing temperatures the shape of the metamolecules does not change) for one hour and the following steps consist of simply increasing the temperature by 50°C with a ramp of 15 min and annealing for another hour. This step is repeated until the desired temperature has been reached. An schematic showing how the process of annealing is supposed to shape the metamolecules is shown in figure 2.

Fig. 2. Steps of the annealing process and how it affects the shape and form of the metamolecules.

2.1.3. Index-matching

The material of choice for index matching was PMMA, with a refractive index of 1.48, which is, compared with PDMS index matching (figure A.1). The process is done by simply drop casting PMMA directly into all the samples and spin coating it at 1000 rev/min. The resulting thin films were approximately of 500 nm thickness.

For the photoluminiscence (PL) analysis SU8 was this time employed for index matching, with a refractive index of 1.57. The chosen polymer was mixed with Rhodamine B (approximately 1% in weight), which is a known organic chemical component commonly used as dye for its fluorescence properties, and then spincoated in the assembly as aforementioned.

2.2. Characterization

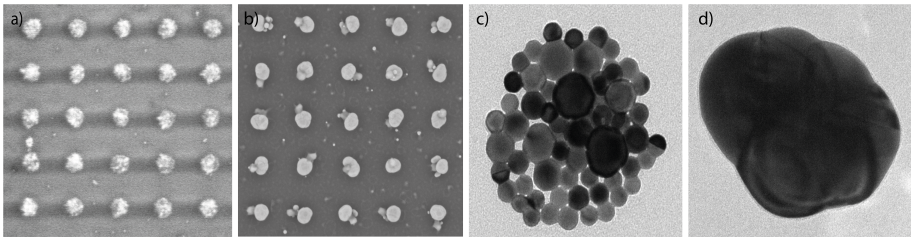

Fig. 3. Micrographs showing the change of the shape of the metamolecules of the assembly with the annealing process. SEM images of the assembly a) without and b) with the annealing process. TEM images of a single metamolecule c) before and d) after the annealing process.

The resulting assemblies were characterized using different microscopy techniques, SEM, TEM and AFM. The SEM micrographs were taken by a SEM QUANTA FEI 200 FEG-ESEM and a High Resolution SEM Magellan 400L. The TEM used was a JEOL JEM1210 (120KV) and for AFM a Keysight 5100. Several micrographs of SEM and TEM were obtained for a

comparison of the shape of the metamolecules before and after annealed assemblies, both with a lattice parameter of 500 nm as seen in figure 3. Along with TEM diffraction patterns (figure A.3) it was concluded that the metamolecules have remained polycrystalline.

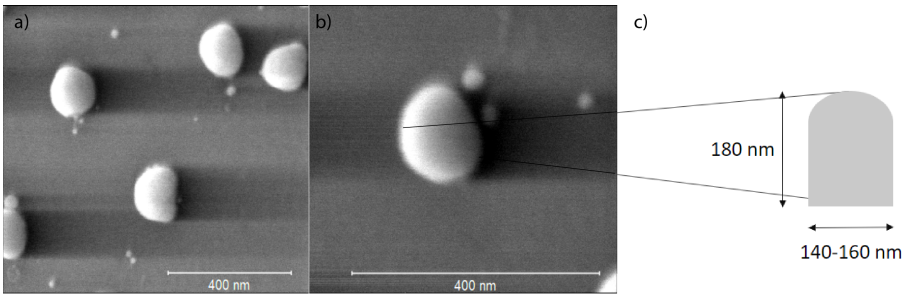

Fig. 4. a), b) Micrographs of an annealed assembly (350°C) tilted 45° and c) the final retrieved shape of the metamolecule.

The final assessment of the metamolecules' shape was done by analysing profiles and 3D models of the AFM micrographs (figure A.4), and tilted SEM images. After annealing an assembly till 350°C we obtain a shape similar to a cylinder with a with a curved facet as it is observable in figure 4. As the temperature is increasing, the shape of the metamolecules barely changes. Therefore, there is no reason to anneal the assemblies any further. The size parameters of this form were the ones used as input in our numerical simulations with FDTD (finite difference in the time domain method). By reproducing the experimental transmittance spectra from the annealed samples we refined the shape of the particle obtained. The final particle shaped is depicted in figure 4c.

2.3. Optical analysis

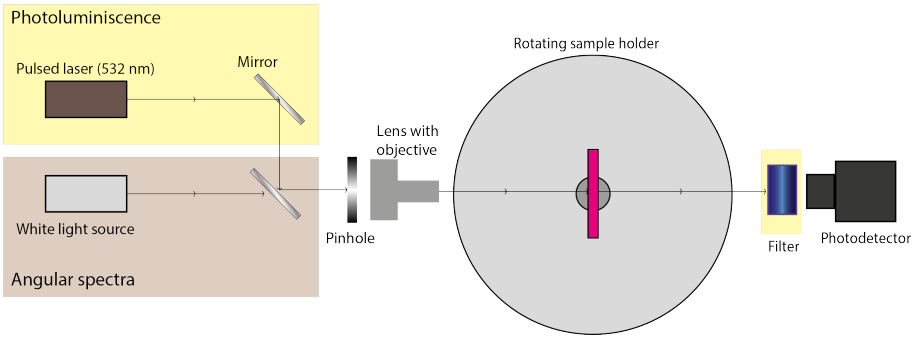

Fig. 5. Schematic of the optical system used to measure the angular spectra and the photoluminiscence.

For a first optical analysis, the transmitted light was measured using a Bruker Fourier transform infrared spectrometer (FT-IR). For the study of the angular response of the samples we used a home build set up as it can be seen in figure 5. The general system is composed of a white light source, then a pinhole followed by an objective lens to focus the light in the center of the rotating sample holder and finally a photo-detector. For the photoluminiscence (PL) measurements a similar system was used with some differences, a pulsed laser of 532 nm was used, together with two mirrors for redirecting the light and an UV filter, set right before the photo-detector. The system was operated by a labView program and the results plotted in Matlab.

3. Results and discussion

In this section, we report the results obtained after doing the optical analysis of the annealed assemblies at different temperatures for comparison after index matching. The first part comprises the FT-IR measurements at normal incidence and the angular measurements; In the second, we compare the experimental results with the simulations. Finally, we report the PLE using the annealed assemblies with Rhodamine B doped SU8 for the index matching.

3.1. Q-factor measurements

We measured the transmittance of annealed assemblies, with a lattice parameter of 500 nm, after the index matching at different temperatures. This was done to compare the transmission profiles and finding an optimal temperature with the sharper resonances. In figure 6 we can see how the resonances change with the temperature and how the assembly at 350°C was considered as being the most optimal.

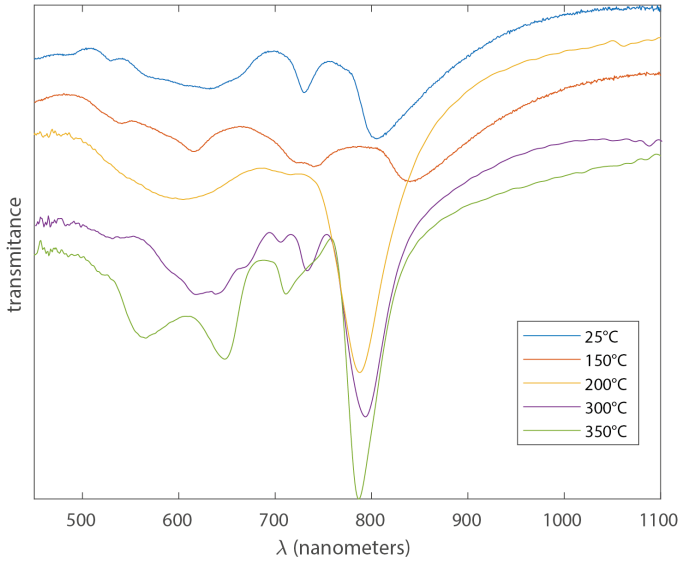

Fig. 6. Transmittance plots at normal incidence for assemblies with different temperatures of annealing.

Additionally, angular spectra measurements were done to get a better comparison and to analyse the behaviour of the fabricated assemblies (figure 7). These angular measurements made appreciable the coupling between the Rayleigh modes and the lattice modes as it was expected for these parameters of lattice [10]. Both figures indicate the tendency towards a sharper resonance as the temperature increases. However, as aforementioned, the shape of the metamolecules does not change, so we remain with the limit temperature of 350°C.

The quality factor, Q-factor, in here was obtained by computing the ratio of the wavelength of the resonance and the full width at half maximum. The highest value calculated was of 22 for the annealed assembly at 350°C, which is an improvement from the Q-factor of 8 the non-annealed (ambient temperature) assembly's resonance. Comparing it with a recent similar work in which a Q factor of 66 was achieved [10], it's an adequate initial result as it is was the first time exploring this kind of metasurface and the effect of the annealing on the plasmonic arrays. We are confident that if we observe an enhancement in the Q factor of these arrays from 8 to 22, this enhancement

will be much higher when starting from plasmonic arrays with a Q factor of 66 as in the case of the cited reference.

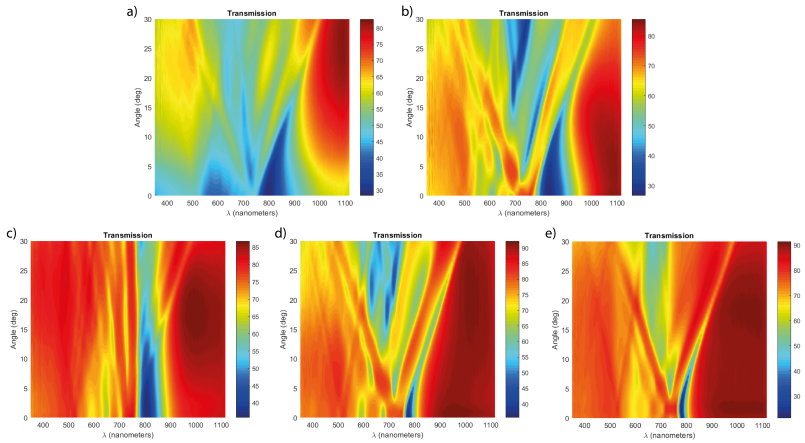

Fig. 7. Transmittance plots for different annealing temperatures, a) 25°C, b) 150°C, c) 200°C, d) 300°C and e) 350°C, with a clear tendency of narrower resonances to higher temperatures.

3.2. Simulations

To analyse the resulting resonances and identify them to a certain component of the electric field, simulations were computed in the FDTD method with the commercial software of Lumerical Solutions Inc. This method solves the Maxwell differential equations in the time domain using spatial grids or lattices, i.e. it samples in space the unknown electric and magnetic fields over a period of time, until finally connecting the physics of the whole system [17].

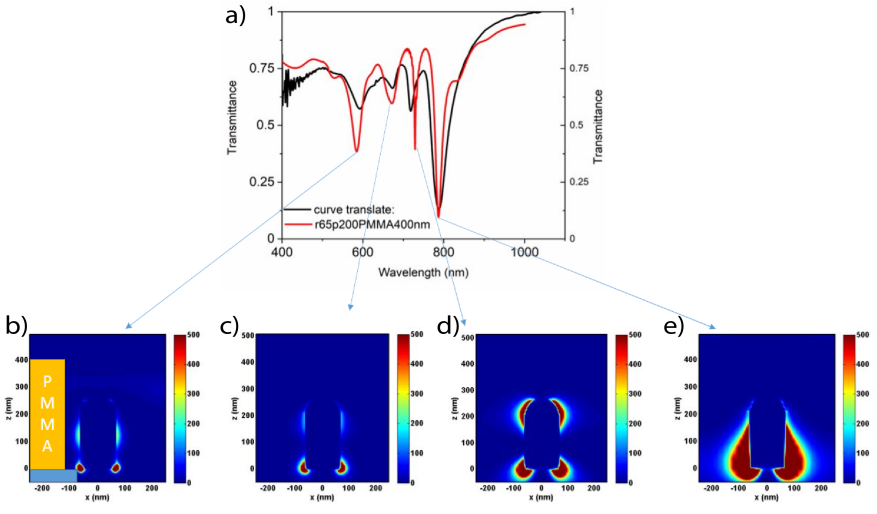

Fig. 8. a) Comparison of transmission plots for the experimental data and the theoretical FDTD simulation together with the b), c), d) and e) field decomposition indicating the origin of each resonance in a determined frequency.

The simulations were carried out using the parameters obtained by the characterization of the metamolecules and the optical parameters of gold retrieved from Johnson and Christy [18]. The experimental/theory comparison can be seen in figure 8 along with the field profiles. We observe an excellent agreement between theory and experiments as the shape of the metamolecule is indeed the origin of the different resonances that are not due the PSLR.

From this last figure we can observe that the sharper resonance (Figure 8e) is due the dipolar contribution of the fields which is the evidently strongest contribution while the other three (figure 8b, c and d) are due the quadrupolar contributions of the field with relatively different weighs. It seems that when the colloids are annealed the final crystalline structure enables the coupling of these "new" modes with the Rayleigh anomalies of the system. For a more profound explanation a more extensive analysis of these modes is needed in addition to a further physical mathematical approach.

3.3. Photoluminiscence characterization.

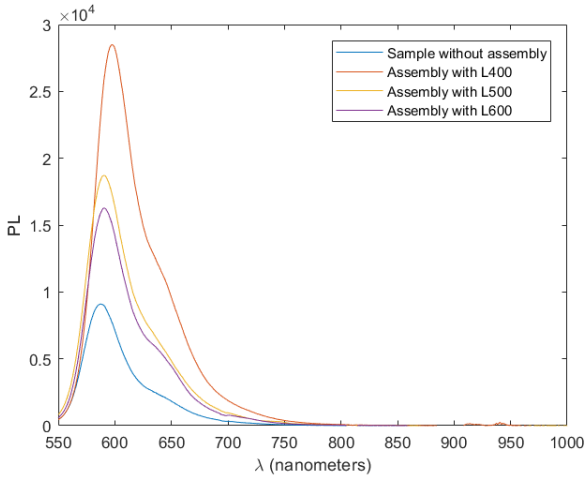

Fig. 9. Photoluminiscence spectra for dye-doped assemblies of different lattice parameters and for a dye-doped blank sample.

The assemblies used used for the photoluminescence were index matched using SU8 instead of PMMA as it is a material previously that was used for rhodamine B doping [19] and it has a similar refractive index (1.57). As the assemblies used in this section were annealed till 350°C the transmission plots are quite similar to the results shown in the previous section.

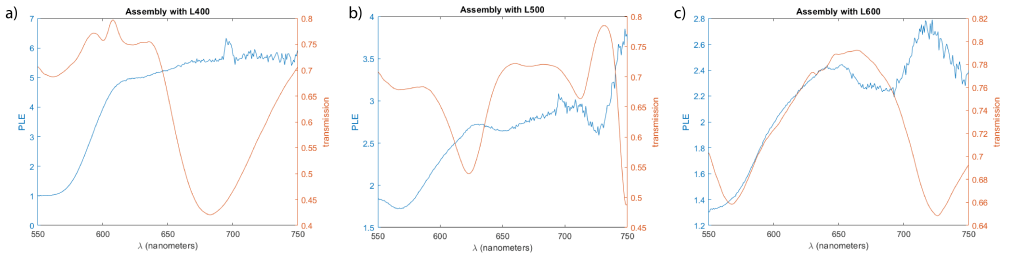

Fig. 10. Overlapped PLE and transmission plots of assemblies with lattice parameters of a) 400, b) 500 and c) 600 nm.

The assemblies index matched with the dye-doped SU8 were put through the prior described PL optical system described ´previoulsy. It is known that rhodamine B has an excitation peak at 546 nm and an emission peak at 568 nm, so the pulsed laser of 532 nm is suitable for a good excitation of the dye. The PL was measured for assemblies of L400, L500 and L600 as the resonances are different for each. The PL of each assembly and a blank sample (without assembly) was measured and plotted in figure 9. It is noticeable that all the samples with assemblies have a considerable higher PL with the L400 having the highest. For finding out why, the photoluminiscence enhancement (PLE) was calculated and plotted together with the transmission spectra of the respective assemblies in figure 10.

The L400 exhibits the higher PLE of the three, which makes sense as it's largest resonance is the closest to the emission of the rhodamine. Nevertheless, the other two give acceptable PLEs, which potentially can be greater if an extensive analysis is made.

It is important to note that other experiments of PL that were made using higher concentrations of rhodamine and power of the laser resulted in the visualization of short times of lasing that lead to the burning of the patterned site of the assembly. The most probable reason is that the LSP resonance of the gold nanoparticles is similar to the laser frequency causing them to burn at high power intensities. An alternative would be to use silver nanoparticles as their LSPR is further into the UV range.

4. Conclusion

In this internship, an extensive experimental and theoretical analysis of annealed gold metamolecules assemblies was presented. Assemblies of polycrystalline metamolecules arranged in periodic arrays were achieved by the method developed by the host group which I learned and an annealing process developed simultaneously. These were characterized by several microscopy techniques and a well-determined shape was then retrieved. An analysis of the optical properties was carried out which lead to an optimal temperature for obtaining sharper resonances, 350°C, with a quality factor of 22. Finally, annealed assemblies were dye-doped and put through a photoluminiscence analysis in which there is an considerable increase of PLE relative to samples without the assembly. As the annealing process yielded adequate results, it was not modified during the project. However, it would be interesting to change annealing parameters in order to have a complete understanding of the process that came to play. On the other hand, the PLE results indicate that also an extensive analysis is needed in order to take advantage of the potential that this kind of metasurfaces could have in several applications, specifically in lasing. The use of different noble metals or a mix of them looks promising as it has never been done in the past and it could improve the results presented in this writing. This work was an exploratory analysis as it is the first time doing the annealing of these type of ordered structures. The results presented here are interesting for using them in further works within the research group.

5. Acknowledgments

I would first like to thank my supervisor, Dr. Agustin Mihi, for this opportunity and for his valuable guidance throughout this project. His insightful feedback and encouragement pushed me to sharpen my thinking and brought my work to a higher level. I would like to acknowledge my colleagues from the ICMAB for letting me use the facilities, providing me with the right tools to complete this study and for being so welcoming. In addition, I would like to thank the Europhotonics program and all the professors for the courses, activities and opportunities they provided. Finally, I would like to thank my colleagues, friends and family for their unconditional support and sympathetic ear.

References

1. M. Meier, P. F. Liao, and A. Wokaun, "Enhanced fields on rough surfaces: dipolar interactions among particles of sizes exceeding the Rayleigh limit," J. Opt. Soc. Am. B **2**, 931 (1985).
2. G. Mie, "Beiträge zur Optik trüber Medien, speziell kolloidaler Metallösungen," Annalen der Physik **330**, 377–445 (1908).
3. J. N. Anker, W. P. Hall, O. Lyandres, N. C. Shah, J. Zhao, and R. P. Van Duyne, "Biosensing with plasmonic nanosensors," (2008).
4. L. YJ, K. J, C. HY, W. C, D. N, S. CE, W. CY, L. MY, L. BH, Q. X, C. WH, C. LJ, S. G, S. CK, and G. S, "Plasmonic nanolaser using epitaxially grown silver film," Sci. (New York, N.Y.) **337**, 450–453 (2012).
5. S. Kawata, Y. Inouye, and P. Verma, "Plasmonics for near-field nano-imaging and superlensing," Nat. Photonics 2009 3:7 **3**, 388–394 (2009).
6. A. HA and P. A, "Plasmonics for improved photovoltaic devices," Nat. materials **9**, 205–213 (2010).
7. L. Scarabelli, D. Vila-Liarte, A. Mihi, and L. M. Liz-Marzán, "Templated Colloidal Self-Assembly for Lattice Plasmon Engineering," (2020).
8. V. G. Kravets, A. V. Kabashin, W. L. Barnes, and A. N. Grigorenko, "Plasmonic Surface Lattice Resonances: A Review of Properties and Applications," Chem. Rev. **118**, 5912–5951 (2018).
9. M. B. Ross, C. A. Mirkin, and G. C. Schatz, "Optical Properties of One-, Two-, and Three-Dimensional Arrays of Plasmonic Nanostructures," J. Phys. Chem. C **120**, 816–830 (2016).
10. P. Molet, N. Passarelli, L. A. Pérez, L. Scarabelli, and A. Mihi, "Engineering Plasmonic Colloidal Meta[U+2010]Molecules for Tunable Photonic Supercrystals," Adv. Opt. Mater. p. 2100761 (2021).
11. D. Dregely, H. Giessen, M. Hentschel, N. Liu, and H. Giessen, "Plasmonic oligomers: the role of individual particles in collective behavior," CLEO:2011 - Laser Appl. to Photonic Appl. (2011), paper QFA5 p. QFA5 (2011).
12. D. Wang, A. Yang, A. J. Hryn, G. C. Schatz, and T. W. Odom, "Superlattice Plasmons in Hierarchical Au Nanoparticle Arrays," ACS Photonics **2**, 1789–1794 (2015).
13. C. Hanske, M. Tebbe, C. Kuttner, V. Bieber, V. V. Tsukruk, M. Chanana, T. A. F. König, and A. Fery, "Strongly Coupled Plasmonic Modes on Macroscopic Areas via Template-Assisted Colloidal Self-Assembly," Nano Lett. **14**, 6863–6871 (2014).
14. C. Matricardi, C. Hanske, J. L. Garcia-Pomar, J. Langer, A. Mihi, and L. M. Liz-Marzán, "Gold Nanoparticle Plasmonic Superlattices as Surface-Enhanced Raman Spectroscopy Substrates," ACS Nano **12**, 8531–8539 (2018).
15. S. Deng, R. Li, J. E. Park, J. Guan, P. Choo, J. Hu, P. J. Smeets, and T. W. Odom, "Ultranarrow plasmon resonances from annealed nanoparticle lattices," Proc. Natl. Acad. Sci. United States Am. **117**, 23380–23384 (2020).
16. M. Bechelany, X. Maeder, J. Riesterer, J. Hankache, D. Lerose, S. Christiansen, J. Michler, and L. Philippe, "Synthesis mechanisms of organized gold nanoparticles: Influence of annealing temperature and atmosphere," Cryst. Growth Des. **10**, 587–596 (2010).
17. W. K. Chen, *The electrical engineering handbook* (2005).
18. P. B. Johnson and R. W. Christy, "Optical Constant of the Nobel Metals," Phys. Rev. B **6**, 4370–4379 (1972).
19. S. Venugopal Rao, A. A. Bettiol, K. C. Vishnubhatla, S. N. Bhaktha, D. Narayana Rao, and F. Watt, "Fabrication and characterization of microcavity lasers in rhodamine B doped SU8 using high energy proton beam," Appl. Phys. Lett. **90**, 1–4 (2007).